Synthesis, Characterization and *in Vitro* Antimicrobial Screening of the Xanthate Derivatives and their Iron(II) Complexes

Mansouri Torshizi, Hassan*+; Zareian Jahromi, Sareh
Department of Chemistry, University of Sistan and Baluchestan, Zahedan, I.R. IRAN

Saeidifar, Maryam
Department of Nanotechnology and Advanced Materials, Materials and Energy Research Center, Karaj, I.R. IRAN

Ghasemi, Ali
Department of Biology and Microbiology, University of Sistan and Baluchestan, Zahedan, I.R. IRAN

Ghaemi, Hamed
Islamic Azad university, Neyshabur branch, Neyshabur, I.R. IRAN

Heydari, Ali
Department of Chemistry, University of Sistan and Baluchestan, Zahedan, I.R. IRAN

ABSTRACT: *Seven reported xanthate ligands and their new Fe(II) complexes of formulaNa[Fe(R-OCSS)$_3$], where R is ethyl-, propyl-, butyl-, pentyl-, Hexyl-, heptyl- and octyl-xanthate have been synthesized. They have been characterized using elemental analysis, molar conductance, FT-IR, UV-Vis and ^{1}H NMR spectroscopic techniques and melting-, decomposition-points for ligands and complexes respectively. All the ligands and their Fe(II) complexes have been evaluated for their antimicrobial activity against four gram-positive bacteria, four gram-negative bacteria and three fungi by agar disc diffusion technique. The MIC values of the compounds exhibited significant antifungal activity but showed lower antibacterial activity. The iron(II) complexes are found to possess higher antimicrobial activity than their counterpart ligands thus improving its antimicrobial efficacy. Hydrocarbon chain length of the ligands coordinated to Fe(II) centers seemed to be important for their antifungal as well as antibacterial activities.*

KEYWORDS: *Xanthate; Fe(II) complex; Antifungal activity; Antibacterial activity*.

***** *To whom correspondence should be addressed.*
+ E-mail: hmtorshizi@hamoon.usb.ac.ir
1021-9986/2017/5/43-8 *8/$/5.80*

INTRODUCTION

The incidence of drug resistance of infectious disease is the main reason for developing safe and efficient antimicrobial compounds. Moreover, fungal and bacterial infections continue to increase rapidly because of the increased number of immunocompromised patients (AIDS, cancer, and transplants) as well as patients undergoing more invasive medical procedures. For these reasons, there is most need to develop new chemical products with antimicrobial activity to the treatment of infectious diseases [1-4].

The role of transition metal complexes in biological and medical sciences has been well established during the past few decades [5]. Synthesis and study of metal complexes with dithio ligands such as dithiocarbamates and xanthates have found application as inhibitors of metal-dependent and sulfhydryl enzymes and have a serious consequence on sulfhydryl enzymes [6-8]. They possess a variety of applications in agriculture such as fungicides, bactericides as well as in the rubber industry like vulcanization accelerators and anti-oxidants [9-13]. In this way, these organosulfur compounds are the main group of fungicides and bactericides used to control approximately 400 pathogens of more than seventy crops registered in many countries. The metal complexes derived from organosulfur derivatives like their ligands have practical application in agriculture, industry, and medicine and has concentrated much attention as an approach to new antimicrobial agent development [14-16].

Keeping in view the potential antimicrobial activity of iron complexes having donor atoms such as nitrogen, oxygen, and sulfur [17-19], in the recent works, we report here the synthesis and study of a series of three n- alkyl xanthate ligands and seven iron complexes as fungicides and bactericides. The goal of this study is to prepare new compounds with better or different antifungal and antibacterial activities than their free ligands, to assess the effect of alkyl chain lengths for ligands and their complexes which are a reflection of their structural activity relationship and the effect of these same compounds on different species of fungal and bacterial strains.

EXPERIMENTAL SECTION

Materials and methods

All the chemicals (ethanol, 1- propanol, 1- butanol, 1- pentanol, 1- hexanol, 1- heptanol, 1- octanol, iron(II) sulfate, carbon disulfide and sodium hydroxide) and solvents were purchased from Merck Chemical Co. and used as received. The microorganisms were provided by the microbiology laboratory culture collection, department of microbiology, Tehran University, Iran.Chloramphenicol, Ampicillin, Clotrimazole, and Ketaconazole were obtained from Daroogar Pharmaceutical Co. Ltd, Tehran Iran.Melting point(for ligands) and decomposition point(for complexes) were carried out using a Unimelt capillary melting point apparatus and were uncorrected. The conductivity measurements of the complexes were carried out on a Systronics conductivity bridge 305. The CHN analysis was performed on Herause CHNO-RAPID elemental analyzer. ^{1}H NMR spectra were recorded on a Brucker DRX-500 Avance spectrometer at 500 MHz in DMSO-d_6 using tetramethylsilane as an internal reference. FT-IR spectra were recorded on a Jasco-460 plus FT-IR spectrometer in the range of 4000 to 400 cm^{-1}usingKBr pellets. UV-Vis spectra were measured on a Jasco UV-Vis-7850 recording spectrophotometer.

Synthesis of ligands

General procedure for R-OCSSNa, R= Et, Pro, But, Pen, Hex, Hep or Oct

The ligands were prepared based on our published methods [6, 8]. Typically, NaOH (4 g, 100 mmol) and corresponding alcohol were mixed to get a homogenous curdy solution. It was then kept in an ice bath and 20 ml (200 mmol) of CS_2 was added drop wise over a period of 30 min with constant stirring. Stirring continued for 1h in an ice bath and 2 h at room temperature. The crude product was dried at 35 $^{\circ}$C and stirred with 30 ml acetone and filtered. To the filtrate, 40 ml diethyl ether was added and kept in the refrigerator overnight. Afterwards, the cream-colored microcrystals were filtered and washed with diethyl ether and dried for 48 h at 35-40 °C. The synthetic route of xanthate ligands is shown in Scheme 1.

Ethyl xanthate sodium salt (Et-xan-Na), propyl xanthate sodium salt (Pro-xan-Na), butyl xanthate sodium salt (But-xan-Na) and the hexyl xanthate sodium salt (Hex-xan-Na) were prepared and characterized using a similar procedure to that we published previously [8]. However, characterization data for pentyl- heptyl- and octyl-xanthate- sodium salts, abbreviated as (Pen-OCSSNa), (Hep-OCSSNa) and (Oct-OCSSNa) respectively are given in the following pages.

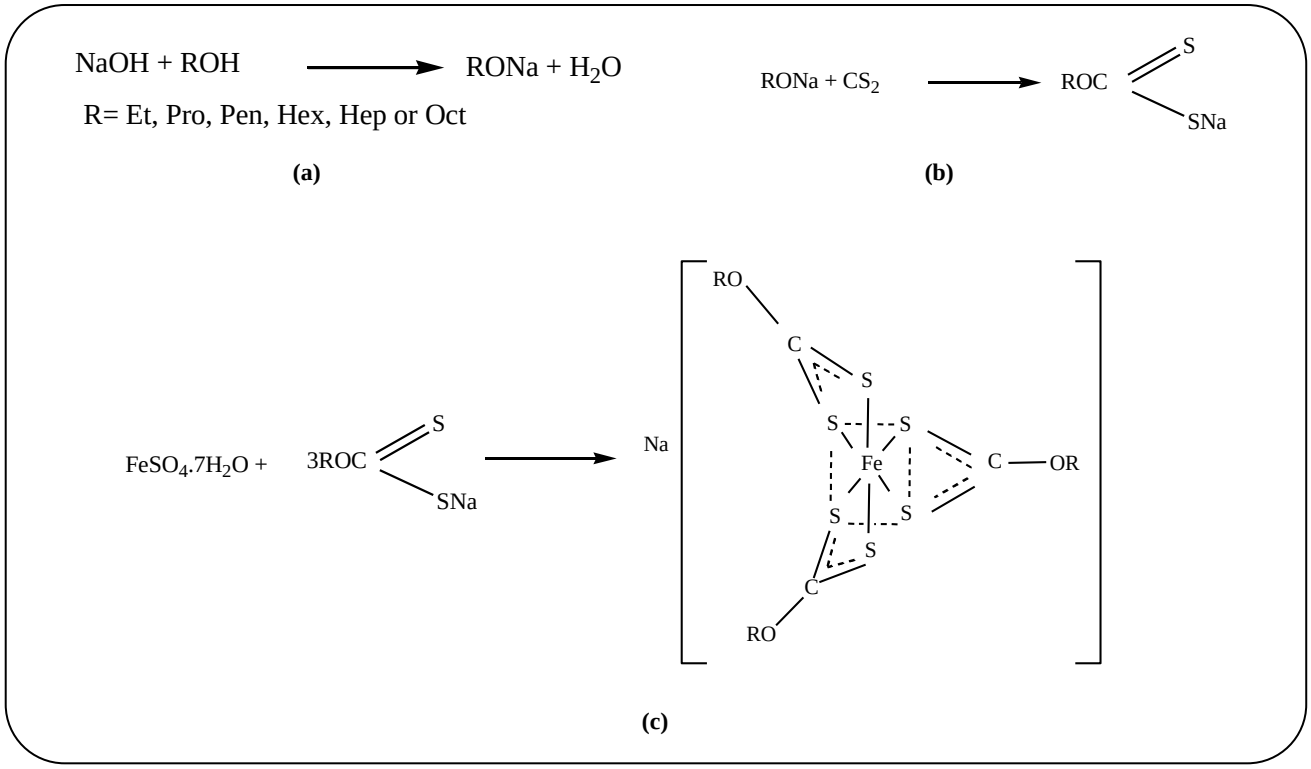

Scheme 1: Synthetic route of the xanthate ligands (a and b) and their Fe(II) complexes (c).

Pen-OCSS-Na:Yield: 0.996 g, (54.3%), m.p.: 79-81 °C. Anal. Calc. for $C_6H_{11}OS_2Na$(MW=186): C, 38.71; H, 5.91; S, 34.41. Found: C, 38.71; H, 5.96; S, 34.51. FT-IR (KBr, cm^{-1}): 1136 (C-O stretching) and 1076 (C-S stretching) [20].^{1}H NMR (500 MHz, DMSO- d_6, 25 °C, S=singlet, d= doublet, t= triplet, sb=singlet broad and m=multiplet) δ (ppm): 0.9 to 0.95 (t, 3H, $\underline{CH_3}$-$(CH_2)_2$-CH_2-CH_2-O], 1.31 to 1.39 [m, 4H, CH_3-$(\underline{CH_2})_2$-CH_2-CH_2-O), 1.58 to 1.69 (m, 2H, CH_3-$(CH_2)_2$-$\underline{CH_2}$-CH_2-O) and 4.21 to 4.27 (t, 2H, CH_3-$(CH_2)_2$-CH_2-$\underline{CH_2}$-O) (Fig-1(D)).

***Hep-OCSS-Na*:**Yield: 0.086 g,(40%), m.p.: 120-124°C.Anal.Calc.for $C_8H_{15}OS_2Na$ (MW=214): C, 44.86; H, 7.01; S, 29.91. Found: C, 44.87; H, 7.02; S, 29.82.FT-IR (KBr, cm^{-1}): 1157 (C-Ostretching) and 1058 (C-S stretching) [20].^{1}H NMR (500 MHz, DMSO-d_6, 25 °C) δ (ppm): 0.84 to 0.87 (t, 3H, $\underline{CH_3}$-$(CH_2)_4$-CH_2-CH_2-O), 1.27 (s possibly m, 8H, CH_3-$(\underline{CH_2})_4$-CH_2-CH_2-O), 1.56 to 1.61 (m, 2H, CH_3-$(CH_2)_4$-$\underline{CH_2}$-CH_2-O) and 4.17 to 4.22 (t, 2H, CH_3-$(CH_2)_4$-CH_2-$\underline{CH_2}$-O) (Fig.1(F)).

Oct-OCSS-Na: Yield: 0.185 g, (81%), m.p.: 146-149°C. Anal. Calc. for $C_9H_{17}OS_2Na$ (M.W= 228): C, 47.37; H, 7.46; S, 28.07. Found: C, 47.38; H, 7.45; S, 28.00.FT-IR (KBr, cm^{-1}): 1140 (C-Ostretching) and 1050 (C-S stretching) [20].^{1}H NMR (500 MHz, DMSO-d_6, 25 °C) δ (ppm): 0.84 to 0.87 (t, 3H, $\underline{CH_3}$-$(CH_2)_5$-CH_2-CH_2-O), 1.27 (s possibly m, 10H, CH_3-$(\underline{CH_2})_5$-CH_2-CH_2-O), 1.55 to 1.60 (m, 2H, CH_3-$(CH_2)_5$-$\underline{CH_2}$-CH_2-O) and 4.16 to 4.21 (t, 2H, CH_3-$(CH_2)_5$-CH_2-$\underline{CH_2}$-O) (Fig.1(G)).

Synthesis of complexes

General procedure for Na [Fe(R-OCSS)$_3$]

An aqueous solution of the corresponding n- alkyl xanthate sodium salt (6 mmol) with constant stirring was added dropwise to an aqueous solution of $FeSO_4.7H_2O$ (0.56 g, 2 mmol). In this volume of water (total 5mL) there was the immediate formation of a dark brown colored precipitate of Na[Fe(R-OCSS)$_3$] complexes. The mixture was stirred for 2-3 h, the solid product filtered, washed with chilled water, acetone and air dried.

In the case of But, Pen, Hex, Hep, and Oct complexes, the product was separated as a dark brown oily layer at the bottom of the beaker which was separated by decanting the water layer and washed with water. The synthetic route of Fe(II) complexes was shown in scheme 1.

Na[Fe(Et-OCSS)$_3$]:Yield: 0.335 g, (76%). It decomposes at242-246°C.Anal. Calc. for $C_9H_{15}O_3S_6FeNa$

(MW=442): C, 24.43; H, 3.39; S, 14.48. Found: C, 24.50; H, 3.41; S, 14.45. FT-IR (KBr, cm^{-1}): 1265 (C-Ostretching) and 1025 (C-Sstretching) [20].^{1}H NMR (500 MHz, $CDCl_3$, 25 ˚C) δ (ppm): 1.41 to 1.56 (m, 3H, $\underline{CH_3}$-CH_2-O), 4.63 to 4.72 (t, 2H, CH_3-$\underline{CH_2}$-O) (Fig.1 (A)). UV-Vis (λ_{max}, nm) (log ε, L mol^{-1} cm^{-1}):283 (4.56) and 250 (4.60). Molar conductivity Λ_m(1×10^{-4} M, H_2O) of the complex is 122.5 Ω^{-1} m^2 mol^{-1}.

Na[Fe(Pro-OCSS)$_3$]:Yield: 0.299 g, (62%). It decomposes at 251-254 ˚C. Anal. Calc. for $C_{12}H_{21}O_3S_6FeNa$(M.W=484): C, 29.75; H, 4.34; S, 13.22.Found: C, 29.10; H, 4.30; S, 13.19. FT-IR (KBr, cm^{-1}): 1263 (C-O stretching) and 1021(C-S stretching) [20]. ^{1}H NMR (500 MHz, $CDCl_3$, 25 ˚C) δ (ppm): 0.97 to 1.10 (m, 3H, $\underline{CH_3}$-CH_2-CH_2-O), 1.72 to 1.94 (m, 2H, CH_3-$\underline{CH_2}$-CH_2-O) and 4.54 to 4.63 (m, 2H, CH_3-CH_2-$\underline{CH_2}$-O) (Fig.1 (B)).UV-Vis (λ_{max}, nm) (log ε, L/mol cm): 283 (4.54) and 250 (4.70). Molar conductivity Λ_m(1×10^{-4} M, H_2O) of the complex is 119 m^2/mol Ω.

Na[Fe(But-OCSS)$_3$]:Yield: 0.362 g, (69%). It decomposes at: 257-259 ˚C. Anal. Calc. for $C_{15}H_{27}O_3S_6FeNa$ (M.W=526): C, 34.22; H, 5.13; S, 6.08.Found: C, 34.19; H, 5.15; S, 6.10. FT-IR (KBr, cm^{-1}): 1264 (C-O stretching) and 1024 (C-S stretching) [20]. ^{1}H NMR (500 MHz, $CDCl_3$, 25 ˚C) δ (ppm): 0.92 to o.98 (t, 3H, $\underline{CH_3}$-CH_2-CH_2-CH_2-O), 1.42 to 1.56 (m, 2H, CH_3-$\underline{CH_2}$-CH_2-CH_2-O), 1.79 to 1.81 (d possibly m, 2H, CH_3-CH_2-$\underline{CH_2}$-CH_2-O) and 4.59 to 4.63 (t, 2H, CH_3-CH_2-CH_2-$\underline{CH_2}$-O) (Fig.1 (C)). UV-Vis (λ_{max}, nm) (log ε, L/mol cm): 300 (4.68) and 258 (4.77). Molar conductivity Λ_m(1×10^{-4} M, H_2O) of the complex is 121 m^2/mol Ω.

Na[Fe(Pen-OCSS)$_3$]:Yield: 0.370 g, (65%). It decomposes at: 263-267 ˚C. Anal. Calc. for $C_{18}H_{33}O_3S_6FeNa$ (M.W= 568): C, 38.03; H, 5.81; S, 11.27. Found: C, 38.00; H, 5.85; S, 11.20. FT-IR (KBr, cm^{-1}): 1262 (C-O stretching) and 1024 (C-S stretching) [20]. ^{1}H NMR (500 MHz, $CDCl_3$, 25 ˚C) δ (ppm): 0.92 to 0.94 (d possibly m, 3H, $\underline{CH_3}$-$(CH_2)_2$-CH_2-CH_2-O), 1.37 to 1.38 (d possibly m, 4H, CH_3-$(\underline{CH_2})_2$-CH_2-CH_2-O), 1.78 to 1.83 (t, 2H, CH_3- $(CH_2)_2$-$\underline{CH_2}$-CH_2-O) and 4.57 to 4.70 (m, 2H, CH_3-$(CH_2)_2$ -CH_2-$\underline{CH_2}$-O)(Fig.1 (D)). UV-Vis (λ_{max}, nm) (log ε, L/mol cm): 283 (4.43) and 242 (4.70). Molar conductivity Λ_m(1×10^{-4} M, H_2O) of the complex is 122 m^2/mol Ω.

***Na[Fe(Hex-OCSS)$_3$]*:**Yield: 0.498 g, (82%). It decomposes at: 266-269 ˚C. Anal. Calc. for $C_{21}H_{39}O_3S_6FeNa$ (M.W= 610): C, 41.31; H, 6.39; S, 10.49. Found: C, 41.35; H, 6.38; S, 10.32. FT-IR (KBr, cm^{-1}): 1257 (C-O stretching) and 1024 (C-S stretching) [20]. ^{1}H NMR (500 MHz, $CDCl_3$, 25 ˚C) δ (ppm: 0.90 (s possibly m, 3H, $\underline{CH_3}$-$(CH_2)_3$-CH_2-CH_2-O), 1.33 (s possibly m, 6H, CH_3-$(\underline{CH_2})_3$-CH_2-CH_2-O), 1.79 (s possibly m, 2H, CH_3-$(CH_2)_3$-$\underline{CH_2}$-CH_2-O) and 4.21 to 4.60 (d possibly m, 2H, CH_3-$(CH_2)_3$-CH_2-$\underline{CH_2}$-O)(Fig.1 (E)). UV-Vis (λ_{max}, nm) (log ε, L/mol cm): 283 (4.20) and 250 (4.54). Molar conductivity Λ_m(1×10^{-4} M, H_2O) of the complex is 118 m^2/mol Ω.

Na[Fe(Hep-OCSS)$_3$]:Yield: 0.427 g, (65%). It decomposes at: 275-279 ˚C. Anal. Calc. for $C_{24}H_{45}O_3S_6FeNa$ (M.W= 652): C, 44.17; H, 5.90; S, 9.82.Found: C, 44.00; H, 6.00; S, 9.86. FT-IR (KBr, cm^{-1}): 1261 (C-O stretching) and 1024 (C-S stretching) [20]. ^{1}H NMR (500 MHz, $CDCl_3$, 25 ˚C) δ (ppm): 0.81 to 0.89 (m, 3H, $\underline{CH_3}$-$(CH_2)_4$-CH_2-CH_2-O), 1.17 to 1.55 (m, 8H, CH_3-$(\underline{CH_2})_4$-CH_2-CH_2-O), 1.67 to 1.85 (m, 2H, CH_3-$(CH_2)_4$-$\underline{CH_2}$-CH_2-O) and 4.57 to 4.69 (m, 2H, CH_3-$(CH_2)_4$-CH_2-$\underline{CH_2}$-O)(Fig.1 (F)).UV-Vis (λ_{max}, nm) (log ε, L/mol cm): 283 (4.32) and 250 (4.66). Molar conductivity Λ_m(1×10^{-4} M, H_2O) of the complex is 117 m^2/mol Ω.

***Na[Fe(Oct-OCSS)$_3$]*:**Yield: 0.389 g, (56%). It decomposes at: 279-282 ˚C. Anal. Calc. for $C_{27}H_{51}O_3S_6FeNa$ (M.W= 694): C, 46.69; H, 7.35; S, 9.22. Found: C, 47.00; H, 7.62; S, 9.28. FT-IR (KBr, cm^{-1}): 1262 (C-O stretching) and 1025 (C-S stretching) [20]. ^{1}H NMR (500 MHz, $CDCl_3$, 25 ˚C) δ (ppm): 0.99 (s possibly m, 3H, $\underline{CH_3}$-$(CH_2)_5$-CH_2-CH_2-O), 1.29 to 1.57 (d possibly m, 10H, CH_3-$(\underline{CH_2})_5$-CH_2-CH_2-O), 1.79 (s possibly m, 2H, CH_3-$(CH_2)_5$-$\underline{CH_2}$-CH_2-O) and 4.59 (s possibly m, 2H, CH_3-$(CH_2)_5$-CH_2-$\underline{CH_2}$-O)(Fig. 1 (G)). UV-Vis (λ_{max}, nm) (log ε, L/mol cm): 283 (4.56) and 250 (4.63). Molar conductivity Λ_m(1×10^{-4} M, H_2O) of the complex is 119 m^2/mol Ω.

Antimicrobial activity

The bioactivity of all these ligands and their iron(II) complexes were screened for their ability to inhibit the growth of the gram-negative bacteria (Escherichia coli, Pseudomonas aeruginosa, Salmonella typhimurium, *Yersinia enterocolitica*, proteus mirabilis), gram-positive bacteria (Staphylococcus aureus, *Enterococcus faecalis*, Bacillus cereus) and two fungal strains

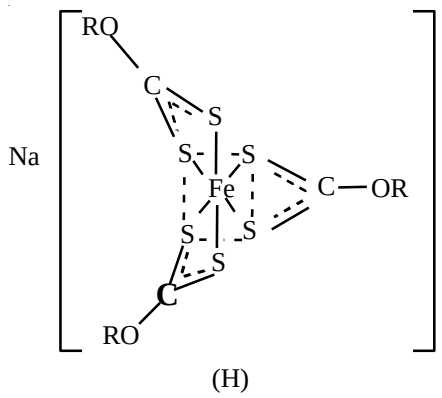

(H)

a b
R= CH_3-CH_2-O-CSSNa (A)

a b c
R=CH_3-CH_2-CH_2-OCSSNa (B)

a b c d
R=CH_3-CH_2-CH_2-CH_2-OCSSNa (C)

a b c d
R=CH_3-$(CH_2)_2$-CH_2-CH_2-OCSSNa (D)

a b c d
R=CH_3-$(CH_2)_5$-CH_2-CH_2-OCSSNa (G)

a b c d
R=CH_3-$(CH_2)_4$-CH_2-CH_2-OCSSNa (F)

a b c d
R=CH_3-$(CH_2)_5$-CH_2-CH_2-OCSSNa (G)

Fig. 1: Proposed structures and 1H NMR numbering scheme of N- alkyl xanthate ligands (A→G) and their Fe(II) complexes (H).

(*Aspergillusniger*and Candida albicans). Chloramphenicol and Ampicillin standards were used as a reference for bacteria to evaluate the potency of the tested compounds, while clotrimazole and Ketaconazole were used for fungi as standards. Antimicrobial activities of the synthesized compounds were evaluated using the agar disc diffusion method. The bacteria were first incubated at 35˚C for 24h in nutrient broth (Difco) and the yeasts were incubated in sabouraud dextrose broth (Difco) at 28˚C for 24– 48h. The culture of bacteria and yeasts were injected into Petri dishes (1mL/ 100mL of medium). Then, sterilized nutrient agar and SDA (autoclaved at 121˚C for 30 min and cooled to 45– 50˚C) were homogenously distributed on to the Petri dishes in the amount of 15cm^3 to give a depth of 3– 4 mm. Subsequently; the sterilized blank paper discs (6 mm diameter) impregnated with the test compound (50 µg/mL) in DMF were placed on the solidified medium, which had previously been inoculated with the above organisms. In addition, blank paper disks treated with Chloramphenicol, Ampicillin, Ketaconazole, and Clotrimazole antibiotics were used as positive controls. The plates were preincubated for 1h at room temperature and then the plates injected with yeast were incubated at 28˚C for 24– 48 h, and those injected with bacteria were incubated at 35˚C for 24 h for antifungal and antibacterial activity, respectively. After 24– 48 h, inhibition zones appearing around the discs were measured.Finally, the millimeters of the inhibition zones generated by the complexes were recorded.

Minimum inhibitory concentration (MIC) of the synthesized compounds was also determined by agar dilution method. The MIC was considered to be the lowest concentration of the test substance exhibiting no visible growth of bacteria or fungi on the plate. A specified quantity of the medium (40-50 ˚C) (Nutrient agar for antibacterial activity and sabouraud dextrose agar for antifungal activity) containing a different concentration of the tested compounds (1– 50 µg/mL) were poured into 8 cm plates and allowed to solidify. Then 10 µL of bacterial and fungal suspensions (1.5 × 10^8cfu/mL) were inoculated on each plate and incubated at 35 ˚C for 24– 48 h for bacteria and at 28 ˚C for 48– 72 h for fungi.

RESULTS AND DISCUSSION

Spectral characterization of ligands and iron (II) complexes

Sodium alkyl xanthates are prepared by saturating the corresponding alcohol with NaOH, cooling and then carbon disulfide was dropped dropwise. The light yellow fine crystalline products are stable at room temperature and they are soluble in water. $FeSO_4.7H_2O$ and corresponding sodium n-alkyl xanthate reacted under mild conditions in water to give their xanthate complexes(scheme 1). The obtained results showed the formula for Fe(II) complexes as Na[Fe (R-OSS)$_3$]

where R= ethyl, propyl, butyl, pentyl, hexyl, heptyl, and octyl. The complexes were soluble in 1:1 H_2O-DMF mixture, DMF, and DMSO. They are thermally stable at room temperature and decomposed without melting. Measurements of their molar conductivity in H_2O- DMF (1:1 ratio v/v) indicated Fe(II) complexes to be 1:1 electrolyte [21,22].Attempts at crystallization of the iron complexes were unsuccessful. However, the elemental analysis and spectral studies enable us to predict the structures of the ligands and their complexes.

Elemental analysis and molar conductivity measurements

The satisfactory results between experimental and calculated values for elemental analysis revealed the successful synthesis and purity of synthesized compounds. It also confirmed coordination of the 1:3 metal-to-ligand xanthate derivatives.The molar conductivities of 1×10^{-4} M metal complexes at room temperature were measured in 1:1 ratio of H_2O- DMF solution. These values are in the range of117- 122 cm^2/mol Ω indicating that they are 1:1 electrolyte [22]. It suggests that the Fe ions in the structure of the complexes should be in +2 oxidation state and the three thiol ligands bear -1 each. Thus each complex ion has a total of -1 charge being balanced with Na^+cation (Scheme 1)

IR spectroscopy

The IR spectra of these xanthate complexes showed the characteristic absorptions of R-$OCSS^-$ group in the region ~1142 and ~1060 cm^{-1} for ligands and ~1262 and ~1024 cm^{-1} for metal complexes[23, 24]. Those at approximately 1142– 1262 cm^{-1} are attributable to the stretching vibrations of $\nu_{(COC)asymm}$ group, while the band around 1024– 1060 cm^{-1} belong to the ν_{C-S} vibration [25,26]. The bands due to $\nu_{(COC)asymm}$ group for the free ligands are shifted towards higher frequencies, while the ν_{C-S} undergoes shift towards lower frequency in the complexes indicating involvement of sulfur atoms of R-$OCSS^-$ group in coordination with iron(II) ion [20, 27]. These results explain the shortening of C-O-C bonds and lengthening of C-S bonds which cause the increase and decrease of the frequencies, respectively. Moreover, as reported by Bonati and Ugo for analogous dithiocarbamate complexes, the ν_{C-S} stretching frequencies may be used to distinguish between the monodentate and bidentate behavior of dithiol ligands. In case of monodentatedithio ligands, a doublet peak appears around 1000 cm^{-1} separated by ≥ 20 cm^{-1} which are due to non-equivalence of two C-S stretching vibrations[28]. On the other hand, in case of bidentate dithio ligands, a strong singlet is observed in ~ 1000 cm^{-1} region, which is indicative of symmetrically bound dithiomoiety. In present series of dithio iron complexes, we observed only one strong band at 1024 cm^{-1}, which indicates that all the xanthate ligands are bidentate and symmetrically bonded.

^{1}H NMR spectroscopy

The ^{1}H NMR spectra of the compounds show the characteristic resonances of the R (Et to Oct) groups in the expected aliphatic region which confirm the proposed formulae of the xanthate ligands and complexes. In both ligands and complexes, Et shows two sets, Pro three sets and Bu, Pen, Hex, Hep, and Oct four sets of signals at room temperature(Fig. 2 and spectra in supplementary section). This indicates that the three R groups present in the structure of each of the complexes are equivalent. The coordination of the xanthate ligands with iron (II) invariably produces a downfield shift in the position of their proton signals relative to those of the free xanthate ligands. The extent of this downfield shift decreased regularly with distance from the coordination site. This is due to the electron donation by CSS^- group to iron center. Thus, based on the spectroscopic data, the structures as shown in Fig. 1, were assigned to these ligands and complexes. Further support for the proposed structures come from the ratio of the integrated areas under the peaks of R groups of xanthate protons being 3: 2 for Et, 3: 2: 2 for Pro, 3: 2: 2: 2 for Bu, 3: 4: 2: 2 for Pen, 3: 6: 2: 2 for Hex, 3: 8: 2: 2 for Hep and 3: 10: 2: 2 for Oct. R groups in free ligands as well as complexes. No changes were observed in the ^{1}H NMR spectra of the above complexes dissolved in $CDCl_3$ and recorded after 24 h suggesting no dissociation of xanthate anions.Moreover, as reported by Tsipis and Manoussakis, in case of metal dithiocarbamate complexes, sharp ^{1}H NMR spectra without being split indicate the non-coexistence of mono and bidentate dithiocarbamate ligands[29]. A similar observation was seen for all of our xanthate complexes. Finally, as it can be seen from these spectra, there is no any sign of paramagnetism (broadening of signals) and almost all signals are sharp enough to indicate non-paramagnetic nature of complexes.

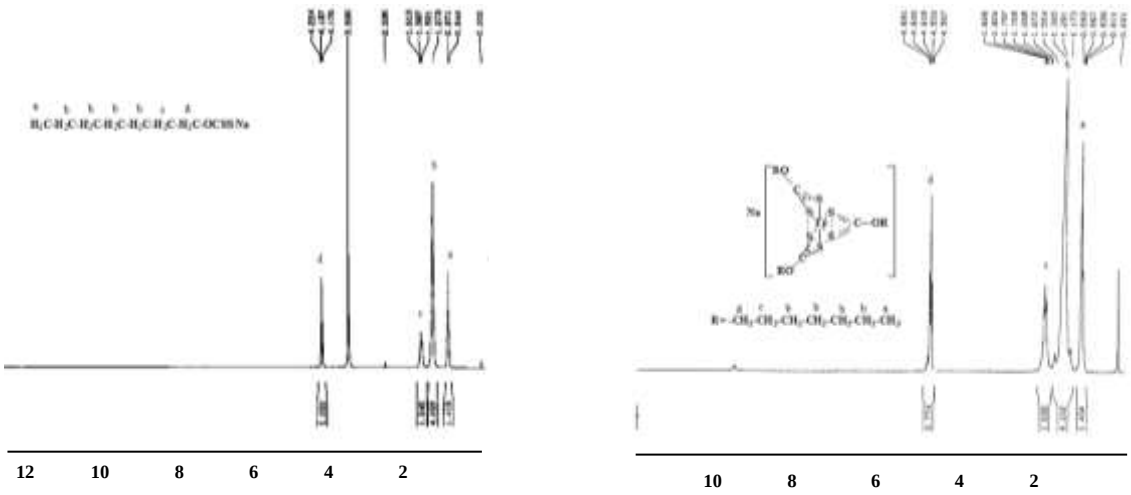

Fig. 2: ^{1}H NMR spectrum of Hep-Xa-Na ligand and its corresponding ^{1}H NMR spectrum of Na[Fe(Hep-Xa)$_3$] complex.

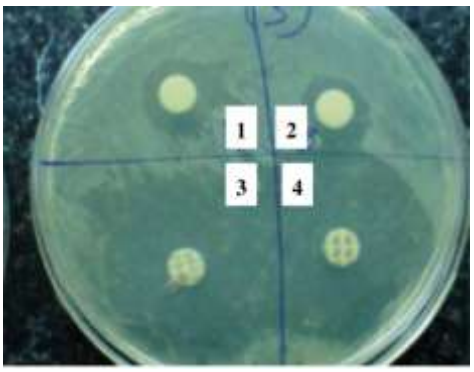

Fig. 3: In vitro sensitivity with E.coli to: (1) Na[Fe(Oct-OCSS)$_3$], (2) Oct-OCSSNa(3) Ampicillin and (4) Chloramphenicol.

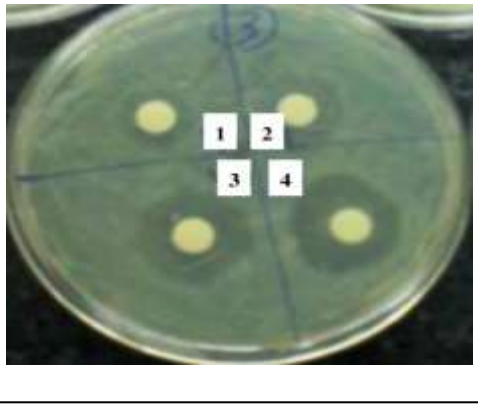

Fig. 4: In vitro sensitivity with B.cereusto: (1) Na[Fe(pen-OCSS)3], (2) pen-OCSS-Na (3) Na[Fe(Hep-OCSS)3] and (4) Hep-OCSS-Na.

UV-Vis spectroscopy

The ligands and their iron complexes show characteristic UV-Vis spectra for the –OCSS$^-$ group. The electronic spectra of ligands exhibit two intense bands appeared sharply at 300 nm and 225 nm which may be assigned to n→π* and π→π* transition of CS_2 groups. Same observations have been made by N. Manav and coworkers for CS_2 groups of dithio ligands[29, 30]. On complexation, these two bands overlapped and shifted to ~ 280 nm (broad) and ~ 250 nm (shoulder), revealing the involvement of CSS$^-$ group in chelate formation. These peaks positions and overlapping are in substantial agreement with those previously recorded by *Jorgensen* [31, 32].

Antimicrobial activity

The antimicrobial activity was assayed using paper disc diffusion method by measuring the zones of inhibition in millimeter and Minimum Inhibitory Concentration (MIC) by agar dilution method. All the compounds were screened *in vitro* for their antibacterial and antifungal activities against a variety of gram-negative and gram-positive bacterial and fungal strains and the results are given in Figs. 4 and 5. Na[Fe(Oct-OCSS)$_3$] complex showed a remarkable activity against *E.coli* (Fig. 3). The inhibition diameter is 17 mm and with a MIC value of 3.0 µg/mL.the inhibition diameter obtained by Na[Fe(Hep-OCSS)$_3$] complex against *B.cereus* is 17 mm and its MIC value is 1 µg/mL (Fig. 4).

Table 1: Minimum inhibitory concentration of ligands(µg/ml) against bacterial and fungal pathogens.

Compound	Name of bacterial pathogens								Name of fungal pathogens	
	S.aureus	*E.fecalis*	*B.cereus*	*E.coli*	*P.aeroginosa*	*S.typhi*	*Y.entroculitica*	*P.mirabilis*	*A.niger*	*C.albicans*
Et-OCSS-Na	21	31	25	20	34	23	31	6	20	2
Pro-OCSS-Na	14	35	12	15	32	20	23	12	18	10
Bu-OCSS-Na	3	24	10	8	14	14	15	13	3	5
Pen-OCSS-Na	5	15	7	6	21	13	18	3	12	3
Hex-OCSS-Na	7	19	3	10	18	12	13	9	1	2
Hep-OCSS-Na	4	9	1	9	10	8	6	1	4	1
Oct-OCSS-Na	5	17	2	3	4	4	20	2	9	1
Chloramphenicol (100 µg/ disc)	0.5	0.2	0.2	0.1	0.4	0.1	0.5	0.1	_	_
Ampicillin (100 µg/ disc)	0.2	0.3	0.1	0.4	0.5	0.1	0.4	0.4	_	_
Ketaconazole (100 µg/ disc)	–	–	–	–	–	–	–	–	0.2	0.1
Clotrimazole (100 µg/ disc)	–	–	–	–	–	–	–	–	0.5	0.2
DMF	0	0	0	0	0	0	0	0	0	0

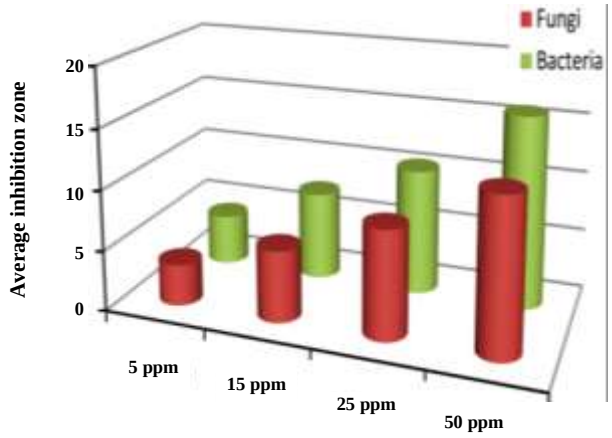

Fig. 5: Comparison of antimicrobial activities of seven Fe(II) complexes at various concentrations (5, 15, 25 and 50 ppm). Fungi and Bacteria indicate average fungi and bacterial activities of seven complexes respectively.

These results show a marked activity against bacterial strains tested. In these studies, four different concentrations of each ligand and iron complexes were selected (5,15,25 and 50 ppm). We observed the maximum inhibitory zones at 50 ppm (Fig. 5). The results of inhibition zones of microbial growth produced by different compound and MIC of the compounds against eight bacteria and two fungi are presented in Tables 1 and 2.

The activity of reference compounds Chloramphenicol, Ampicillin, Ketaconazole, and Clotrimazole for comparison purposes was included. The obtained results show that all synthesized ligands and iron complexes were active against all tested microorganisms with a range of inhibition zones and MIC values, *E. coli* (11-17 mm and 3-28 µg/mL), *P. earuginosa* (8-15 mm and 4-45 µg/mL), *S. typhi* (10-16 mm and 4-30 µg/mL), Y. *enterocolitica*(10-16 mm and 6-40 µg/mL), *P. mirabilis* (11-15 mm and 1-20 µg/mL), *S. aureus* (7-15 mm and 5-30 µg/mL), *E. faecalis* (8-13 mm and 9-42 µg/mL), *B.cereus* (10-17 mm and 1-30 µg/mL), *A. niger* (11-18 mm and 1-25 µg/mL) and *C. albicans* (13-18 mm and 1-12 µg/mL). These experimental results indicate that the iron (II) complexes are more active than their counterpart ligands which may be due to bidentate coordination (chelation) of xanthate ligands with Fe(II) center via two sulfur atoms. Such an increased activity for the metal chelates as compared to the free ligand can be explained on the basis of chelation theory. Chelation reduces the polarity of the metal ion which is due to neutralization of positive charges on Fe(II) ion with negative charges on sulfur atoms of threedithiol ligands as well as partial sharing of p-electron of donor groups over the chelate ring. Such chelation could increase the liposolubility of the iron complexes, which subsequently

Table 2: Minimum inhibitory concentration of Fe(II) complexes(μg/ml) against bacterial and fungal pathogens.

Compound	Name of bacterial pathogens								Name of fungal pathogens	
	S.aureus	*E.fecalis*	*B.cereus*	*E.coli*	*P.aeroginosa*	*S.typhi*	*Y.entroculitica*	*P.mirabilis*	*A.niger*	*C.albicans*
Na[Fe (Et-OCSS)$_3$]	21	31	25	20	34	23	31	6	20	2
Na[Fe (Pro-OCSS)$_3$]	14	35	12	15	32	20	23	12	18	10
Na[Fe (But-OCSS)$_3$]	3	24	10	8	14	14	15	13	3	5
Na[Fe (Pen-OCSS)$_3$]	5	15	7	6	21	13	18	3	12	3
Na[Fe (Hex-OCSS)$_3$]	7	19	3	10	18	12	13	9	1	2
Na[Fe (Hep-OCSS)$_3$]	4	9	1	9	10	8	6	1	4	1
Na[Fe (Oct-OCSS)$_3$]	5	17	2	3	4	4	20	2	9	1
Chloramphenicol (100 μg/ disc)	0.5	0.2	0.2	0.1	0.4	0.1	0.5	0.1	_	_
Ampicillin (100 μg/ disc)	0.2	0.3	0.1	0.4	0.5	0.1	0.4	0.4	_	_
Ketaconazole (100 μg/ disc)	–	–	–	–	–	–	–	–	o.2	0.1
Clotrimazole (100 μg/ disc)	–	–	–	–	–	–	–	–	0.5	0.2
DMF	0	0	0	0	0	0	0	0	0	0

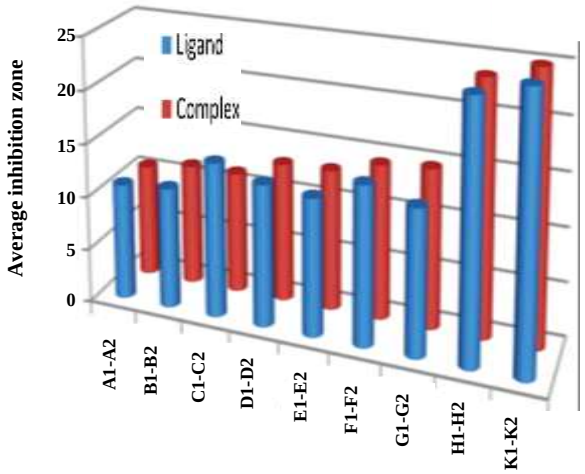

Fig. 6: Antimicrobial activity of seven xanthate sodium salts and their corresponding Fe(II) complexes at 50 ppm, A1: Et-OCSS-Na, A2: Na[Fe (Et-OCSS)$_3$], B1: Pro-OCSS-Na, B2: Na[Fe (Pro-OCSS)$_3$], C1: But-OCSS-Na, C2: Na[Fe (But-OCSS)$_3$], D1: Pen-OCSS-Na, D2: Na[Fe (Pen-OCSS)$_3$], E1: Hex-OCSS-Na, E2: Na[Fe (Hex-OCSS)$_3$], F1: Hep-OCSS-Na, F2: Na[Fe (Hep-OCSS)$_3$], G1: Oct-OCSS-Na, G2: Na[Fe (Oct-OCSS)$_3$], H1: Ampicillin, H2: Ampicillin, K1: Chloramphenicol, K2: Chloramphenicol

favor permeation through the lipid layer of the cell membrane. The mode of action of the complexes may also involve the formation of hydrophobic interaction through alkyl groups of the compounds with active centers of the cell constituents resulting in the interference with normal cell processes.

However, it is interesting that the biological activity of the synthesized compounds is enhanced upon increasing the hydrocarbon chain length presented in the structure of the ligands and their Fe(II) complexes, suggesting that nature of the alkyl group attached to the xanthate moiety plays an important role on the potential activities of these products. Moreover, the Na[Fe(Hep-OSS)$_3$] and Na[Fe(Oct-OSS)$_3$] presented the best antimicrobial activities on all the tested strains (Fig. 6). In comparison, two series of compounds showed better antifungal activity than antibacterial. In addition, the antifungal activities of iron complexes are better than xanthate sodium salts. However, all compounds had low antimicrobial activity against the microorganisms cultures used in this study as compared to the standard antifungal and antibacterial antibiotics.

CONCLUSIONS

A series of seven n-alkyl xanthate sodium salts and their Fe(II) complexes were prepared. Their structures were established by analytical, spectroscopic and non-spectroscopic techniques. All ligands and their iron(II) complexes were screened for their antimicrobial activity against several bacteria and pathogenic fungi. The results

indicated that almost all of the compounds exhibited significant antifungal activity but showed lower antibacterial activity. The iron(II) complexes are more active than their counterpart ligands. The study on structural-activity relationships of these xanthate ligands and corresponding complexes indicated that the hydrocarbon chain length seemed to be important for antimicrobial activities. These activities improved by the increase in the chain length of hydrocarbon moieties.

Acknowledgments

Financial assistance from the Research Council of University of Sistan and Baluchestan is gratefully acknowledged.

Received: Nov. 31, 2016 ; Accepted: Jan. 23, 2017

REFERENCES

[1] Antonio F.S., Débora F.B., Lis R.V. F., Natália A.C., Geziel R.A., Margareth B., Alberto A.C., Ademir N., Daniela C.M.R., Ademir D.A., Study of the Antimicrobial Activity of Metal Complexes and Their Ligands Through Bioassays Applied to Plant Extracts, *Rev. Bras. Farmacogn*., **24**: 309-315 (2014).

[2] Bouchoucha A., Terbouche A., Zaouani M., Derridj F., Djebbar S., Iron and Nickel Complexes with Heterocyclic Ligands: Stability, Synthesis, Spectral Characterization, Antimicrobial Activity, Acute and Subacute Toxicity, *J. Trace Elem. Med Biol.*,**27**: 191-202 (2013).

[3] Sabounchei S.J., Pourshahbaz M., Salehzadeh S., Bayat M., Karamian R., Asadbegy M., Khavasi H.R., New Chlorine Bridged Vinuclear Silver(I) Complexes of Bidentate Phosphorus Ylides: Synthesis, Spectroscopy, Theoretical and Anti-Bacterial Studies, *Polyhedron*, **85**: 652-664 (2015).

[4] Sharma A., Jain A., Saxena S., The Structure–Activity Relationship of Some Hexa coordinated dimethyl Tin(IV) Complexes of Fluorinated β-diketone/ β-Diketones and Sterically Congested Heterocyclic β-Diketones, *Appl. Organomet. Chem.*, **29**: 499-508 (2015).

[5] Kiran T., Prasanth V.G., Balamurali M.M., Vasavi C.S., Munusami P., Sathiyanarayanan K.I., Pathak M., Synthesis, Spectroscopic Characterization and in *Vitro* Studies of New Heteroleptic Copper (II) Complexes Derived From 2-Hydroxy Napthaldehyde Schiff's Bases and N, N Donor Ligands: Antimicrobial, DNA Binding and Cytotoxic Investigations, *Inorg. Chim. Acta*., **433**: 26-34 (2015).

[6] Alijanianzadeh M., Saboury A.A., Mansuri-Torshizi H., Haghbeen K., Moosavi-Movahedi A.A., The Inhibitory Effect of Some New Synthesized Xanthates on Mushroom Tyrosinase Activities, *J. Enzyme Inhibition and Medicinal Chemistry*, **22**: 239-246 (2007).

[7] Hanif M., Chohan Z.H., Synthesis, Spectral Characterization and Biological Studies of Transition Metal(II) Complexes with Triazole Schiff Bases, *Appl. Organomet. Chem*., **27**: 36-44 (2012).

[8] Saboury A.A., Alijanianzadeh M., Mansouri- Torshizi H., The Role of Alkyl Chain Length in the Inhibitory Effect n-alkyl Xanthates on Mushroom Tyrosinase Activities, *Acta Biochim. Pol*., **54**: 183-191 (2007).

[9] Geraldo M.D., Daniele C.M., Camila A.C., Jaqueline A.F.d., Isabella P.F., Eucler B.P., James L.W., Solange M.S.V.W., Klaus K., Isolda C.M., Heloisa B., Synthesis, Characterisation and Biological Aspects of Copper(II) Dithiocarbamate Complexes, $[Cu\{S_2CNR(CH_2CH_2OH)\}_2]$, (R=Me, Et, Pr and CH_2CH_2OH), *J. Mol. Struct*, **988**: 1-8 (2011).

[10] Anthony C.E., Damian C.O., Cyril U., Eno E.E., Mixed Ligand Complexes of N-Methyl-N-phenyl Dithiocarbamate: Synthesis, Characterisation, Antifungal Activity, and Solvent Extraction Studies of the Ligand, *Bioinorg. Chem. Appl*.**, 2015**: 1-8 (2015).

[11] Syed Q.S., Mohammad R.K., Synthesis of ^{99m}TcN-Clinafloxacin Dithiocarbamate Complex and Comparative Radiobiological Evaluation in Staphylococcus Aureus Infected Mice, *World J. Nucl. Med*., **13**: 154-158 (2014).

[12] Mohammad T., Cr(III), Mn(II), Fe(III), Co(II), Ni(II), Cu(II) and Zn(II) Complexes with Diisobutyl dithiocarbamato Ligand, *E-J. Chem*., **8**: 2020-2023 (2011).

[13] Saad E.A., Hasan A.M., Synthesis and Characterization of Mn(II), Fe(II) and Co(II) Complexes with 4-Hydroxypiperidinedithiocarbamate and their Adducts with Neutral Bases, *Raf. J. Sci*., **25**: 53-61 (2014).

[14] Mohammad T., Mohammad A., Investigation on Transition Metal Complexes with Sulphur and Nitrogen Containing Ligand Derived from Diethylamine, *Asian J. Chem*., **22**: 2465-2467 (2010).

[15] Nabipour H., Synthesis of a New Dithiocarbamate Cobalt Complex and Its Nanoparticles with the Study of Their Biological Properties, *Int. J. Nano. Dim*., **1**: 225-232 (2011).

[16] Núñez C., Fernández-Lodeiro A., Fernández-Lodeiro J., Carballo J., Capelo J.L., Lodeiro C., Synthesis, Spectroscopic Studies and in Vitro Antibacterial Activity of Ibuprofen and Its Derived Metal Complexes, *Inorg. Chem. Commun*., **45**: 61-65 (2014).

[17] Xu B., Kong X.L., Zhou T., Qiu D.H., Chen Y.L., Liu M.S., Yang R.H., Hider R.C., Synthesis, Iron(III)-Binding Affinity and in Vitro Evaluation of 3-Hydroxypyridin-4-One Hexadentate Ligands as Potential Antimicrobial Agents, *Bioorg. Med. Chem. Let*., **21**: 6376-6380 (2011).

[18] PramanikH.A.R., Paul P.C., MondalP., Bhattacharjee C.R., Mixed Ligand Complexes of Cobalt(III) and Iron(III) Containing N_2O_2-Chelating Schiff Base: Synthesis, Characterisation, Antimicrobial Activity, Antioxidant and DFT Study, *J. Mol. Struct*., **1100**: 506-512 (2015).

[19] Abdel- Rahman L.H., El- Khatib R.M., Nassr L.A.E., Abu- Dief A.M., Ismael M., Seleem A.A., Metal Based Pharmacologically Active Agents: Synthesis, Structural Characterization, Molecular Modeling, CT-DNA Binding Studies and in Vitro Antimicrobial Screening of Iron(II) Bromosalicylidene Amino Acid Chelates, *Spectrochim. Acta A.*, **117**: 366-378 (2014).

[20] Nakamoto K., "Infrared and Raman Spectra of Inorganic And Coordination Compound", 4th ed. New York. John Wiley and sons. (1986).

[21] Damian C.O., Tanvir A., Christien A.S., Fe(II) and Fe(III) Complexes of N-ethyl-N-phenyl Dithiocarbamate: Electrical Conductivity Studies and Thermal Properties, *Electrochimica Acta*, **127**: 283-289 (2014).

[22] Narges A., Hassan M.T., Maryam N., Farshad H. Sh., Cytotoxicity of Diimine Palladium (II) Complexes of Alkyldithiocarbamate Derivatives on Human Lung, Ovary and Liver Cells**,** *I. J. Pharm. Res*., **11**: 689-695 (2012).

[23] Nabipour H., Ghammamy S., Ashuri Sh., Aghbolagh Z. Sh., Synthesis of a New Dithiocarbamate Compound and Study of Its Biological Properties, *Org. Chem. J*., **2**: 75-80 (2010).

[24] Jayaraju A., Musthak Ahamad M., Rao R.M., Sreeramulu J., Synthesis, Characterization and Biological Evaluation of Novel Dithiocarbamate Metal Complexes, *Der. Pharma. Chemica*., **4**: 1191-1194 (2012).

[25] Mansouri Torshizi H., Saeidifar M., Khosravi F., Divsalar A., Saboury A.A., Hassani F., DNA Binding and Antitumor Activity of α-Diimineplatinum(II) and Palladium(II) Dithiocarbamate Complexes, *Bioinorg. Chem. Appl*., **2011**: 1-11 (2011).

[26] Yahui Z., Zhao C., Yongdan C., Chuanyao S., FTIR Studies of Xanthate Adsorption on Chalcopyrite, Pentlandite and Pyrite Surfaces, *J. Mol. Struct*., **1048**: 434-440 (2013).

[27] Marion G., BöttcherH.-C., Karlheinz S., Synthesis and Structural Characterization of bis-Cyclometalated Complexes $[M(ptpy)_2(S_2COCH_3)]$ (M=Rh, Ir; ptpy=2-(p-tolyl)pyridinato)**,** *Inorganica. Chim. Acta*., **394**: 363-366 (2013).

[28] Nicholas G. S., Eric A.S., Ian R.Sh., Benjamin L.I., Bryan D., Sylvanna V.K., Benjamin F. Gh., Atta M.A., Eric C.B., Synthesis of Zinc and Cadmium O-Alkyl Thiocarbonate and Dithiocarbonate Complexes and a Cationic Zinc Hydrosulfide Complex, *Inorganica. Chimica. Acta.*, **386**: 83-92 (2012).

[29] Chauhan H.P.S., Sapana J., Jaswant C., Synthetic, Spectral, Thermal and Powder X-Ray Diffraction Studies of Bis(Oalkyldithiocarbonato-S,S') Antimony(III)dialkyldithiocarbamates, *Spectrochim Acta A.*, **136**: 1626-1634 (2015).

[30] Yu-Wen L., Shu-Tao L., Facile Synthesis and Antifungal Activity of Dithiocarbamate Derivatives Bearing an Amide Moiety, *J. Serb. Chem. Soc.*, **80**: 1367-1374 (2015).

[31] Loth M., Meddah B., TirTouil A., Len C., Verstraete W., Antifungal Activity of Synthesized Dithiocarbamate Derivatives on Fusariumoxysporum f sp. Albedinisin Algeria, *J. Chem. Pharm. Res*., 7: 49-53 (2015).

[32] Yamini Y., Tamaddon T., Sensing of Iron by Solid Phase Spectrophotometry, *Iran. J. Chem.Chem. Eng. (IJCCE)*, **21**: 91-96 (2002).